A COMPARATIVE STUDY BETWEEN FIELD ORIENTED CONTROL AND SLIDING MODE CONTROL FOR DFIG INTEGRATED IN WIND ENERGY SYSTEM

M. ALLAM*[,1], B. DEHIBA[1], M. ABID[1], K. MOUILAH[1], and Y. DJERIRI[2]

Department of Electrical Engineering, University Djillali Liabes of Sidi Bel Abbes, Algeria, 22000
[1]Interaction REseau COnvertisseur Machines - IRECOM- Laboratory
[2]Intelligent Control & Electrical Power Systems- ICEPS- Laboratory
***allam2010@live.fr**

***Abstract**: This paper presents a modeling and sliding mode control of a doubly fed induction machine (DFIM) integrated in wind energy system for independent control of active and reactive power. For a comparative study, the independent control of active and reactive power is ensured in the first step by conventional controllers (PI) and the second step by sliding mode controllers (SMC). Finally, the performance of the system are tested and compared by simulation in terms of reference tracking, and robustness based on MATLAB / SIMULINK software.*

***Keywords**: Doubly fed induction generator, sliding mode control, Vector control, wind energy.*

1. Introduction

Wind energy is the most promising renewable source of electrical power generation for the future. Many countries promote the wind power technology through various national programs and market incentives. Wind energy technology has evolved rapidly over the past three decades with increasing rotor diameters and the use of sophisticated power electronics to allow operation at variable speed [1-2].

Variable-speed turbines are typically based on a doubly fed induction generator (DFIG), with the stator is usually connected directly to the three-phase grid; the rotor is also connected to the grid but via a transformer and two back-to-back converters (Fig.1). Usually, the rotor-side converter controls the active and reactive power and the grid side converter controls the DC-link voltage and ensures operation of the converter at a unity power factor [3].

The control of DFIG has been well developed, one of the most popular control techniques is the vector control (VC) or flux orientation control (FOC) associated with classical (PI) controllers. The active and reactive power can be regulated by separately controlling the d-axis and q-axis rotor current components. Actually the main drawback of FOC is the unstable system and sensitivity to machine parameters [4-5].

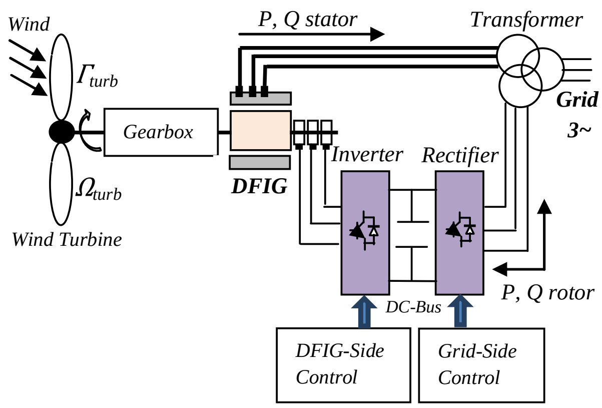

Fig.1 Block of variable speed wind turbine system with a DFIG.

In the area of the control of the electric machines, the research works are oriented more and more towards the application of the modern control techniques. These techniques are the fuzzy control, the adaptive control, and the variable structure control. The aim of this paper is to apply a Variable Structure Control (VSC), called also the sliding mode control (SMC) of the DFIG.

The use of this control mode can be justified by the high performances required by DFIG and the robustness of the controller.

In this work, first, a wind turbine system is presented and its characteristics are depicted to estimate its dynamics and performances in different operating conditions. Then, a SMC of the DFIG used to control independently the active and reactive powers between the stator of and the grid is proposed and tested on a wind turbine equipped with a DFIG of 10 kW.

2. Model and Equations of Wind Turbine

The relation between the wind speed and mechanic power, delivered by the wind turbine, can be described by the following equation:

$$P_{turb} = C_p(\lambda, \beta)\frac{\rho \pi R^2 v^3}{2} \quad (1)$$

with:

$$\lambda = \frac{\Omega_{turb} R}{v} \quad (2)$$

Where: C_p: power coefficient; λ: relative speed; β: pitch angle (*deg*); *R*: radius of turbine; *v*: wind speed (*m/s*); Ω_{turb}: turbine speed (*rd/s*); ρ: air density *(1.225 kg.m*$^{-3}$*)*.

According to Betz, the power coefficient C_p cannot be greater than 16/27 or 0.59 [6-7-8-9].

The torque produced by the turbine is expressed in the following way:

$$\Gamma_{turb} = P_{turb} / \Omega_{turb} \quad (3)$$

A typical relationship between C_p and λ is shown in Fig.2. It is clear from this figure that there is a value of λ for which C_p is maximized thus maximizing the power for a given wind speed. Because of the relationship between C_p and λ, as the turbine speed that gives a maximum output power. This is shown in Fig.3 for various wind speeds.

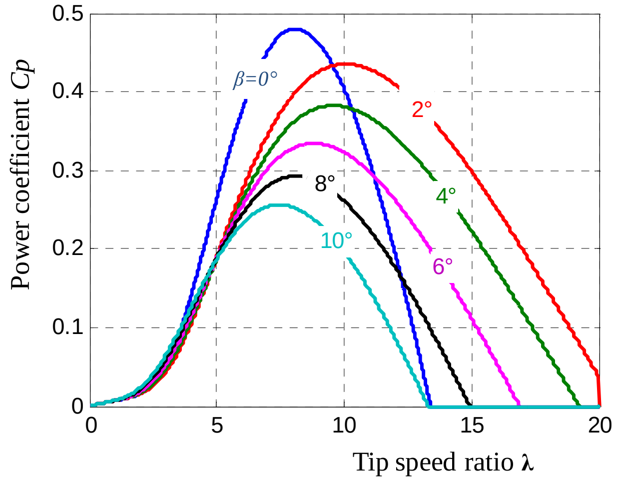

Fig.2 Power coefficient *Cp* as a function of β and λ.

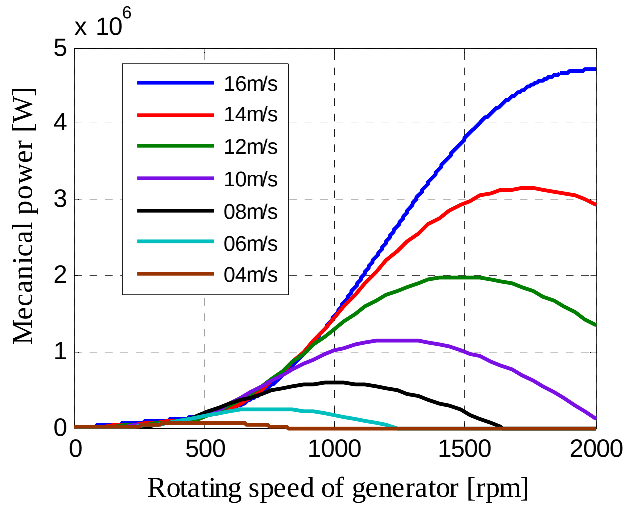

Fig.3 Mechanical power of the wind turbine.

3. Modeling of the DFIG

The dynamic model of doubly fed induction machine in *d-q* frame can be represented by the following equations: [5-6]

3.1 Electrical equations

$$\begin{cases} V_{ds} = R_s I_s + \dfrac{d\varphi_{ds}}{dt} - \omega_s \varphi_{qs} \\ V_{qs} = R_s I_{qs} + \dfrac{d\varphi_{qs}}{dt} + \omega_s \varphi_{ds} \end{cases} \quad (4)$$

$$\begin{cases} V_{dr} = R_r I_{dr} + \dfrac{d\varphi_{dr}}{dt} - (\omega_s - \omega_r)\varphi_{qr} \\ V_{qr} = R_r I_{qr} + \dfrac{d\varphi_{qr}}{dt} + (\omega_s - \omega_r)\varphi_{dr} \end{cases} \quad (5)$$

3.2 Magnetic equations

$$\begin{cases} \varphi_{ds} = L_s I_{ds} + M I_{dr} \\ \varphi_{qs} = L_s I_{qs} + M I_{qr} \end{cases} \quad (6)$$

$$\begin{cases} \varphi_{dr} = L_r I_{dr} + M I_{ds} \\ \varphi_{qr} = L_r I_{qr} + M I_{qs} \end{cases} \quad (7)$$

3.3 Mechanical equation

The fundamental equation of dynamics to determine the evolution of the mechanical speed from total mechanical torque applied to the rotor Γ_{mec}:

$$J\frac{d\Omega_{mec}}{dt} = \Gamma_{mec} = \Gamma_{turb} - \Gamma_{em} - f_r \Omega_{mec}$$

(8)

Where the electromagnetic torque of DFIG (Γ_{em}) can be written as a function of stator fluxes and rotor currents:

$$\Gamma_{em} = P\frac{M}{L_s}\left(I_{qr}\varphi_{ds} - I_{dr}\varphi_{qs}\right) \tag{9}$$

Where: s / r are stator/rotor subscript; V / I: voltage/current; φ: flux; R: resistance; M: mutual inductance; L: inductance; ω_r / ω_s: rotor/stator frequency; f_r: viscous friction; Ω_{mec}: mechanical speed of the DFIG; P: number of the pairs of poles; J: Moment of inertia.

4. Field Oriented Control of the DFIG

In order to easily control the production of electricity by the DFIG, we will carry out an independent control of active and reactive powers by orientation of the stator flux [7-8].

By choosing a reference frame linked to the stator flux, rotor currents will be related directly to the stator active and reactive power. An adapted control of these currents will thus permit to control the power exchanged between the stator and the grid. If the stator flux is linked to the d-axis of the frame (Fig.4) we have [10-11]:

$$\varphi_{ds} = \varphi_s \text{ and } \varphi_{qs} = 0 \tag{10}$$

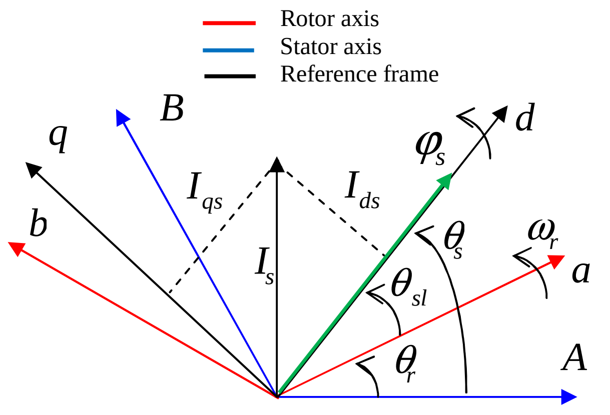

Fig.4 Diagram of the stator flux oriented with d-axis.

The electromagnetic torque equation (9) is then written:

$$\Gamma_{em} = p\frac{M}{L_s}I_{qr}\varphi_{ds} \tag{11}$$

By substituting equation (10) in equation (6), the following rotor flux equations are obtained:

$$\begin{cases} \varphi_{ds} = L_s I_{ds} + M I_{dr} \\ 0 = L_s I_{qs} + M I_{qr} \end{cases} \tag{12}$$

The grid is assumed to be stable and consequently φ_{ds} constant. By neglecting the stator resistance of the DFIG, we obtained:

$$\varphi_s = \frac{V_s}{\omega_s} \tag{13}$$

Where: V_s is the RMS value of the grid voltage. The active and reactive powers of the DFIG can be expressed by:

$$\begin{cases} P_s = V_s I_{qs} \\ Q_s = V_s I_{ds} \end{cases} \tag{14}$$

Using equation (12), a relation between the stator and rotor currents can be established:

$$\begin{cases} I_{ds} = -\dfrac{M}{L_s} I_{dr} + \dfrac{\varphi_s}{L_s} \\ I_{qs} = -\dfrac{M}{L_s} I_{qr} \end{cases} \tag{15}$$

Or from the rotor currents by:

$$\begin{cases} P_s = -V_s \dfrac{M}{L_s} I_{qr} \\ Q_s = -V_s \dfrac{M}{L_s} I_{dr} + V_s \dfrac{\varphi_s}{L_s} \end{cases} \tag{16}$$

The relationship between the rotor currents and voltages are established and will be applied to control the generator by the following equations:

$$\begin{cases} V_{dr} = R_r I_{dr} + \left(L_r - \dfrac{M^2}{L_s}\right)\dfrac{dI_{dr}}{dt} - g\omega_s\left(L_r - \dfrac{M^2}{L_s}\right) I_{qr} \\ V_{qr} = R_r I_{qr} + \left(L_r - \dfrac{M^2}{L_s}\right)\dfrac{dI_{qr}}{dt} + g\omega_s\left(L_r - \dfrac{M^2}{L_s}\right) I_{dr} + g\dfrac{MV_s}{L_s} \end{cases} \tag{17}$$

Where: g: is the rotor slip.

The resulting bloc diagram of the DFIG is presented in Fig. 5.

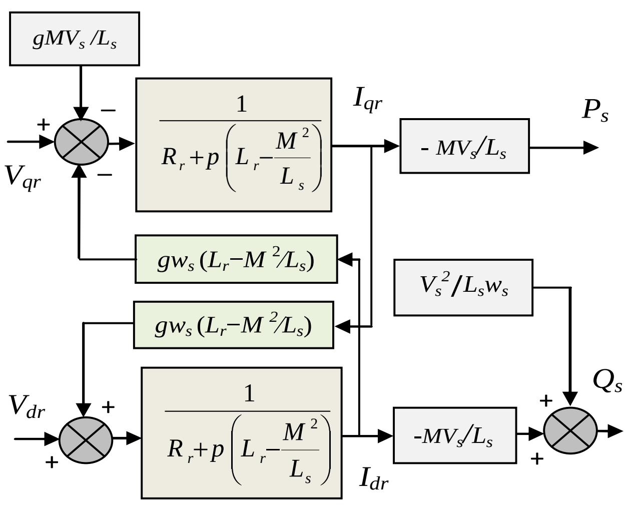

Fig. 5 Block diagram of the DFIG.

5. Sliding Mode Control

5.1 General concepts

The sliding mode control knows a big success these last years. It is due to the implementation simplicity and the robustness with regard to the system uncertainties and the external disturbances.

The SMC consists to return the state trajectory towards the sliding surface and to develop it above, with a certain dynamics up to the equilibrium .Its design consists mainly to determine three stages. [12-13].

5.1.1 The switching surface choice

For a non-linear system represented by the following equation:

$$\dot{X} = f(X,t)+g(X,t)\,u(X,t);\; X \in R^n, u \in R \quad (18)$$

Where: *f(X, t); g (X, t)* are two continuous and uncertain non-linear functions, supposed limited.

We take the general equation to determine the sliding surface, proposed by J.J. Slotine [14-15], given by:

$$S(X)=\left(\frac{d}{dt}+a\right)^{n-1} e \;;\; e = X^d - X \quad (19)$$

Where: *e:* error on the signal to be adjusted; *a*: positive coefficient; *n:* system order; X^d: desired signal; *X:* state variable of the control signal.

5.1.2 Convergence condition

The convergence condition is defined by the Lyapunov equation [12]; it makes the surface attractive and invariant

$$S(X)\dot{S}(X) \le 0 \quad (20)$$

5.1.3 Control Calculation

The control algorithm is defined by the relation [16-17]

$$u = u^{eq} + u^n \quad (21)$$

With:

$$u^n = u^{\max} Sat(S(X)/\varphi) \quad (22)$$

$$Sat(S(X)/\varphi)=\begin{cases} sign(S) & if\ |S|\rangle\varphi \\ S/\varphi & if\ |S|\langle\varphi \end{cases} \quad (23)$$

Where: *u*: control signal; u^{eq}: equivalent control signal; u^n: switching control term; sat ($S(X)/\varphi$): saturation function; φ: threshold width of the saturation function.

5.2 Application of SMC to the DFIM

5.2.1 Active power control

To control the power, the surface expression of the active power control has the form:

$$S(P) = (P_s^{ref} - P_s) \quad (24)$$

Taking its derivative and replacing it in the active power P_s expression (15) we get:

$$\dot{S}(P) = (\dot{P}_s^{ref} + V_s \frac{M}{L_s} \dot{I}_{qr}) \quad (25)$$

Replacing V_{qr} by $V_{qr} = V_{qr}^{eq} + V_{qr}^{n}$, the control appears clearly in the following equation:

$$\dot{S}(P) = (\dot{P}_s^{ref} + V_s \frac{M}{L_s L_r \sigma}((V_{qr}^{eq} + V_{qr}^{n}) - R_r I_{qr}) \quad (26)$$

With: $\sigma = 1 - M^2 / L_s L_r$, σ: Leakage coefficient.

During the sliding mode and in steady state, we have:

$$S(P) = 0, \quad therefore \quad \dot{S}(P) = 0, \quad and \quad V_{qr}^{n} = 0$$

The equivalent control amount V_{qr}^{eq} is found from the previous equations and written as:

$$V_{qr}^{eq} = -\dot{P}_s^{ref} \frac{\sigma L_s L_r}{V_s M} + R_r I_{qr} \quad (27)$$

During the convergence mode, so that the condition $S(P)\dot{S}(P) \le 0$ is verified, we set:

$$\dot{S}(P) = -V_s \frac{M}{\sigma L_s L_r} V_{qr}^{n} \quad (28)$$

And consequently, the switching term is given by:

$$V_{qr}^{n} = KV_{qr}\ sign(S(P)) \quad (29)$$

To verify the system stability condition, the parameter KV_{qr} must be positive.

To reduce any possible overshoot of the reference voltage V_{qr}, it is often useful to add a Voltage limiter which is expressed by:

$$V_{qr}^{lim} = V_{qr}^{max}\, sat(P) \quad (30)$$

5.2.2 Reactive power control

To control the power, the surface expression of the reactive power control has the form:

$$S(Q) = (Q_s^{ref} - Q_s) \quad (31)$$

Taking its derivative and replacing it in the active power Q_s expression (15) we get:

$$\dot{S}(Q) = \dot{Q}_s^{ref} - \left(-V_s \frac{M}{L_s} \dot{I}_{dr}\right) \quad (32)$$

Replacing V_{dr} by $V_{dr} = V_{dr}^{eq} + V_{dr}^{n}$, the control appears clearly in the following equation:

$$\dot{S}(Q) = \dot{Q}_s^{ref} + V_s \frac{M}{L_s L_r \sigma}(V_{dr} - R_r I_{dr}) \quad (33)$$

During the sliding mode and in steady state, we have: $S(Q) = 0$, *therefore* $\dot{S}(Q) = 0$, *and* $V_{dr}^{n} = 0$

The equivalent control amount V_{dr}^{eq} is found from the previous equations and written as:

$$V_{dr}^{eq} = -\dot{Q}_s^{ref} \frac{\sigma L_s L_r}{V_s M} + R_r I_{dr} \quad (34)$$

During the convergence mode, so that the condition $S(Q)\dot{S}(Q) \le 0$ is verified, we set:

$$\dot{S}(Q) = -V_s \frac{M}{\sigma L_s L_r} V_{dr}^{n} \quad (35)$$

And consequently, the switching term is given by:

$$V_{dr}^{n} = KV_{dr}\ sign(S(Q)) \quad (36)$$

To verify the system stability condition, the parameter KV_{dr} must be positive.

To reduce any possible overshoot of the reference voltage V_{dr}, it is often useful to add a voltage limiter which is expressed by:

$$V_{dr}^{lim} = V_{dr}^{max}\ sat(Q) \quad (37)$$

To illustrate the control performance of SMC, sliding mode controller applied to DFIG, a block diagram of the system is proposed in Fig.6.

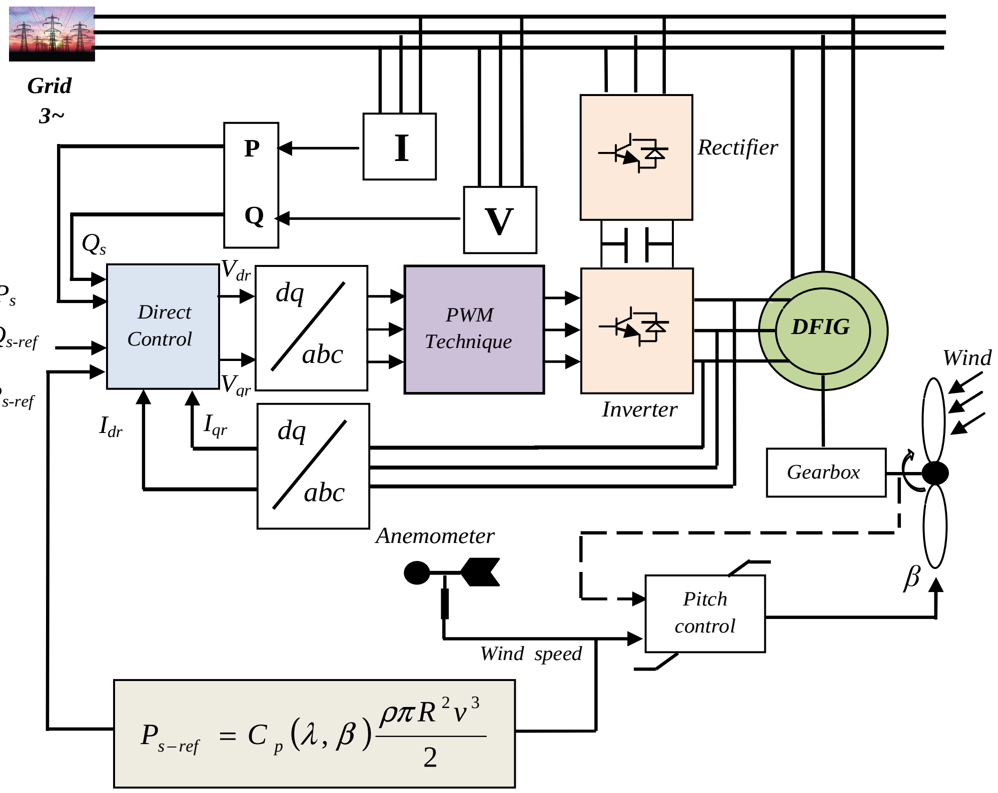

Fig.6 Schematic diagram of SMC strategy for DFIG.

6. Validation of the Proposed Control

In this part, simulations are investigated with a10kW DFIG connected to a 400V/50Hz grid (appendix), by using the MATLAB/SIMULINK software. The both control strategies FOC and SMC are simulated, tested and compared in terms of power reference tracking, robustness against machine parameters variations.

The results plotted in the following figures show the powers generated when reference signals are applied. Fig. 7 shows the responses of the system with the conventional controller (PI), whereas Fig.8 shows the responses with sliding mode controller (SMC), and then fig.9 shows the wind speed variation effect on the active and reactive power.

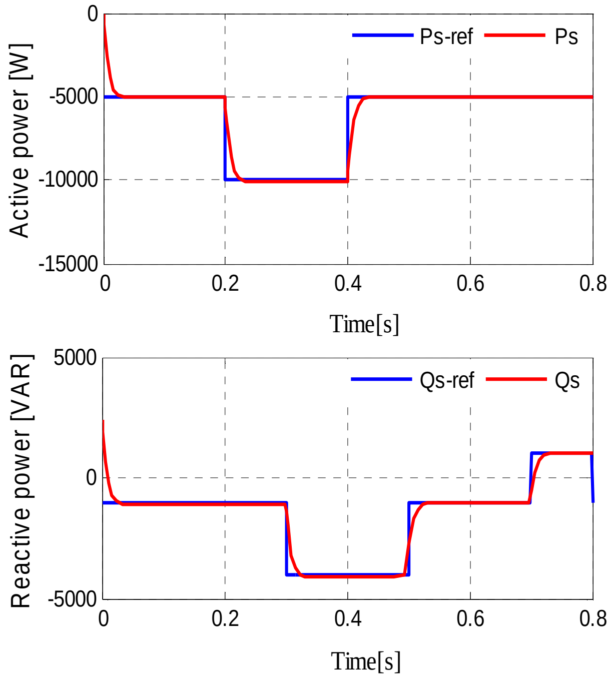

Fig.7 System responses with conventional controller (PI).

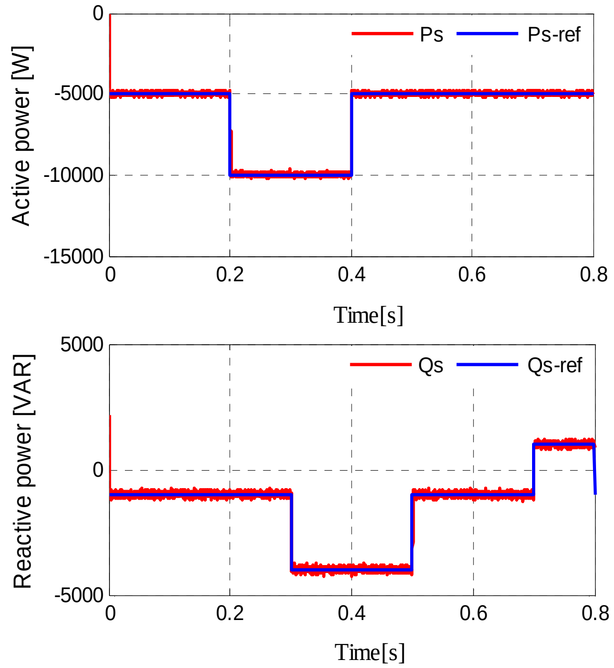

Fig.8 System responses with sliding mode controller (SMC).

According to the Fig.7 and Fig.8 we can see that the power references are followed by the generator both for active and reactive power.

The active power of the stator side is negative, which means that the network in this case is a receiver of the energy supplied by the DFIG, reactive power is adjusted according to the network requirements.

(PI)

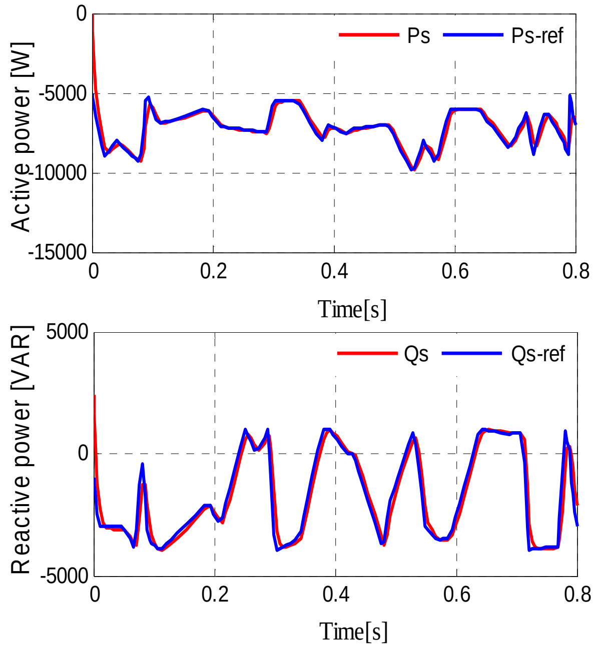

(SMC)

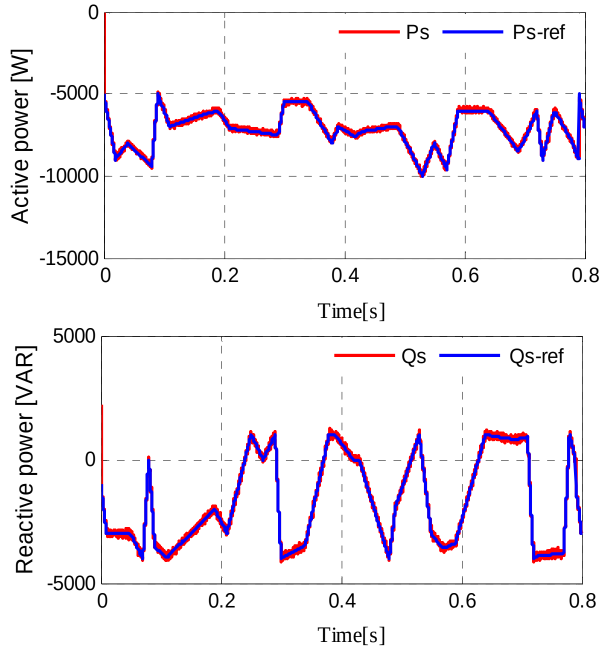

Fig.9 The wind speed variation effect on the active and reactive power.

In the wind power generation system, the DFIG is required to operate at variable speed, for this aim, the required active and reactive power references may also be variable.

Under this circumstance, the active and reactive power of the DFIG follows the power reference calculated from the wind speed. This active power is limited by the generator nominal power (10kW).

6. 1 robustness tests

The Fig.10 represents a comparison between the robustness of the tow controllers: PI and SMC with parametric variations L_s, L_r, R_r and M of -20% and +20% of their nominal's values.

(a) : -20%

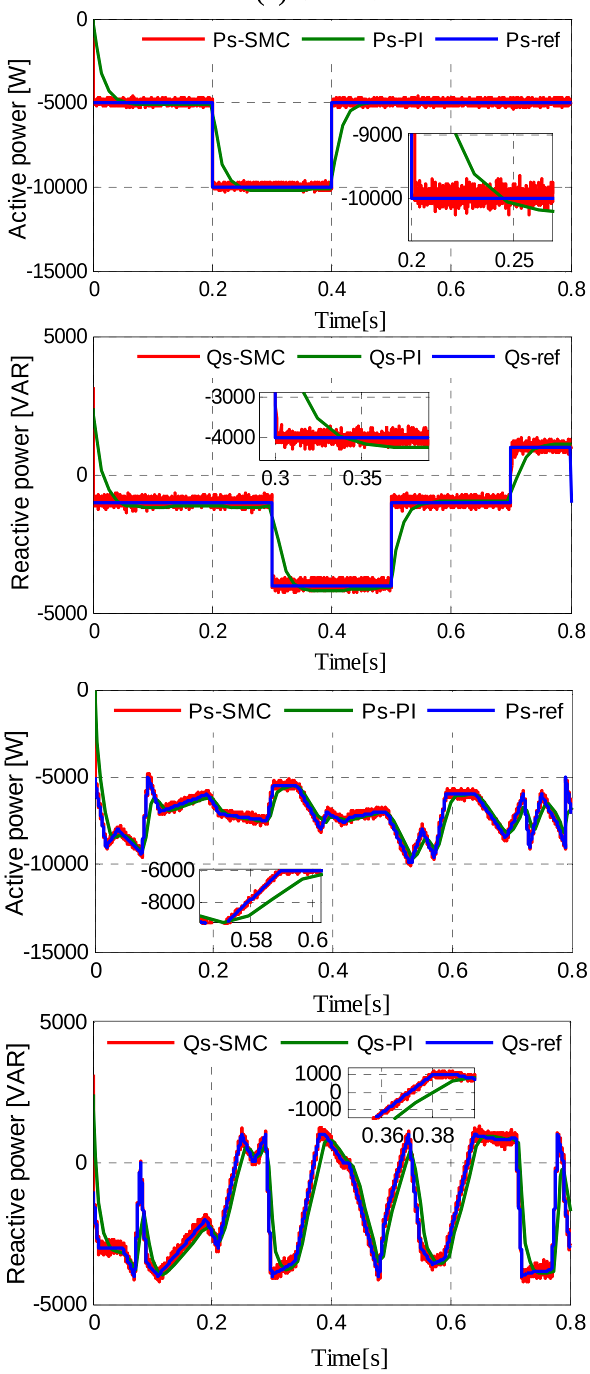

(b) : +20%

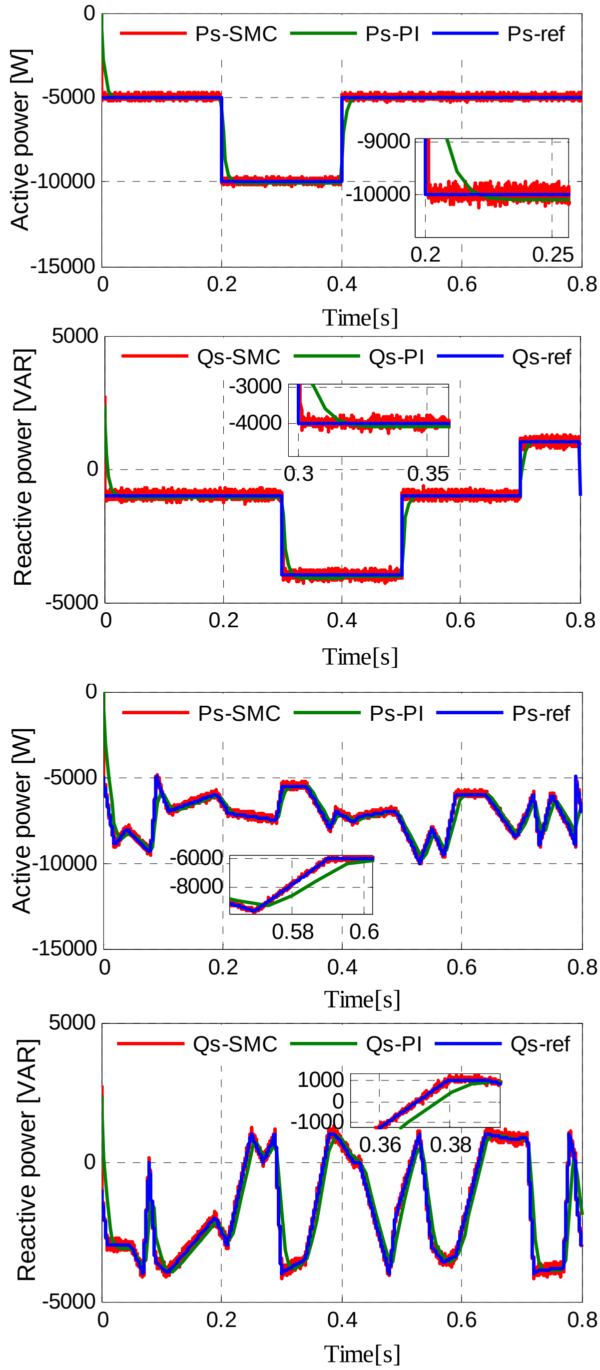

Fig.10 Comparison of robustness between of direct control with (PI) and (SMC).

From the obtained results (Fig.10-a) and (Fig.10-b), we find that FOC strategy can provide good performances and robustness by using sliding mode controller, in terms of response time (Table.1) and reference tracking (Table.2), compared to the FOC with PI controller.

Table. 1 Comparison of response times

	tr (P_s)		tr (Q_s)	
	-20%	+20%	-20%	+20%
PI	35 ms	29 ms	46 ms	40 ms
SMC	0.32 ms	0.30 ms	0.15 ms	0.13 ms

Table. 2 Comparison of static errors

	ΔP_s (%)		ΔQ_s (%)	
	-20%	+20%	-20%	+20%
PI	2.30 (230W)	2.05 (205W)	1.80 (180VAR)	1.55 (155VAR)
SMC	0.085 (8.5W)	0.075 (7.5W)	0.035 (3.5VAR)	0.025 (2.5VAR)

6.2 Power factor control

In this part the stator reactive power reference will be maintained zero to ensure unity power factor at the stator side in the aim to optimize the quality of the energy produced on the grid. The active power reference should allow keeping the power coefficient optimal Fig.11.

(a)

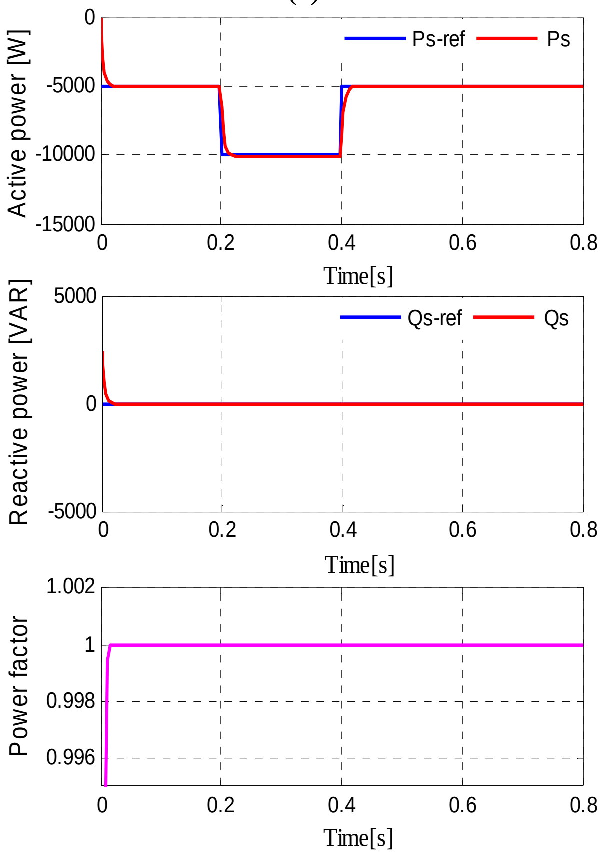

(b)

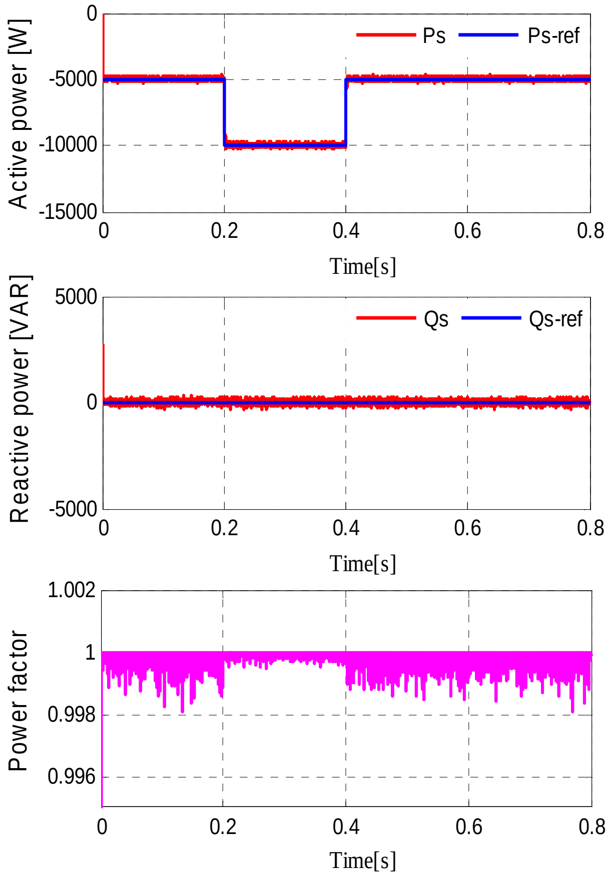

Fig.11 Power factor control

We can say that the control of active power for wind generator is perfectly realized a unity power factor (cosφ = 1) for vector control (Fig.11- a) and sliding mode control (Fig. 11- b).

7. Appendix

Table 3. Doubly fed induction generator parameters

Rated power, P_n	10 kW
Stator rated voltage, V_s	230/400 V
Rated current, I_n	20/30 A
Stator rated frequency, f	50 Hz
Stator resistance, R_s	0.455 Ω
Rotor resistance, R_r	0.19 Ω
Rotor inductance, L_s	0.07 H
Rotor Inductance, L_r	0.0213 H
Mutual inductance, M	0.034 H
Number of pair of poles, p	2
Moment of inertia, J	0.031 Kg.m^2
viscous friction, f_r	0.00114 Kg.m^2/s

8. Conclusion

This paper has presented a comparative study between two controllers of active and reactive powers for DFIG integrated in wind energy system, the first one is a Proportional-Integral (PI) controller and the second is a Sliding Mode (SM) controller based Field Oriented Control (FOC) strategy.

Simulation results show the optimized performances of the FOC strategy based a sliding mode controller. Through the response characteristics, we observe high performances in terms of response time and reference tracking without overshoots. The decoupling, the stability and the convergence towards the equilibrium are assured. Furthermore, this regulation presents a high dynamic response, and it's more robust against parameters variation of the DFIG versus the conventional PI controller.

9. References

1. Report. :*The wind barometer; solar systems*, Journal of Renewable Energy, No.183, European Union, February 2008.
2. O., Anaya-Lara, N., Jenkins, J., Ekanayake, P., Cartwright, M., Hughes.: *Wind Energy Generation*, Wiley, 2009.
3. Petersson, A.: *Analysis, modeling and control of doubly fed induction generators for wind turbines*. PhD thesis, Champers University of Technology, Sweden,2005.
4. Arifujjaman, M. : *Vector control of a DFIG based wind turbine,* Journal of Electrical & Electronics Engineering, No.9,2009, Vol.2, pp.1057-1065.
5. Boyette, A., Poure , P., Saadate , S.: *Direct and indirect control of a Doubly Fed Induction Generator wind turbine including a storage unit*. In: 32th edition of Industrial Electronics Conference IECON', IEEE, France, 2006, pp. 2517-2522.
6. Müller,S.: *Doubly fed induction generator systems*.IEEE Industry Applications Magazine, No.3,2002, vol. 8, pp. 26-33.
7. Poitiers, F., Toufik, B., Machmoum, A.: *Advanced control of a doubly-fed induction generator for wind energy conversion*. Electric Power Systems Research,No.79, 2009, pp. 1085-1096.
8. Djoudi,A. : *Robust exploitation of a wind turbine based on a doubly fed asynchronous machine*, No.4,2012, vol.15, pp.20-29.
9. Cárdenas,R., Peña, R.: *Sensorless vector control of induction machines for variable-speed wind energy applications,* IEEE Trans. Energy Conversion, No. 1, 2004, vol. 19, pp. 196-205.
10. Hopfensperger,B., Atkinson, D. J., and Lakin, R. : *Stator-flux-oriented control of a doubly fed induction machine with and without position encoder*. IEE Proc.Electr. Power Applications, No.4, vol.147, 2000, pp. 241-250.
11. Tapia.A, Tapia.G, Ostolaza.J, and Sáenz.J.R.: *Proportional–integral regulator based approach to wind farm reactive power management for secondary voltage control*, IEEE Trans. Energy Conversion, No. 2, 2007, vol. 22, pp. 488-498.
12. Buhler,H. : *Control by sliding mode*, Presses Polytechnic romandes, Lausanne, 1986.
13. Dehiba,B. : *Adaptive control by sliding mode an electric actuator AC pilot vectorrially*, PhD thesis in Electrical Engineering, Sidi Bel-Abbes university, Algeria, 2006.
14. Slotine, J.J., Li,E.: *Applied nonlinear control*, Prence Hall, USA, 1998.
15. Slotine.J.J.: *Sliding controller design for nonlinear systems, IGC*, No.2, 1984, vol.40, pp.421-434.
16. Utkin,V.I.: *Sliding mode control design principles and applications to electric drives*, IEEE Trans. Ind. Elec.,No.1, 1993, vol. 40, pp.23-36.
17. Serhoud, H., Benattous, D.: *Sensorless Sliding Power Control of Doubly Fed Induction Wind Generator Based on MRAS Observer*, World Academy of Science, Engineering and Technology., No.56, 2011, pp. 920-925.